Photoemission electron microscopy for connectomics

Kevin M. Boergens*[1], Gregg Wildenberg*[2,3], Ruiyu Li[4,5], Lola Lambert[2], Amin Moradi[6], Guido Stam[6], Rudolf Tromp[6,7], Sense Jan van der Molen[6], Sarah B. King[4,5], Narayanan Kasthuri[2,3]

[1] Department of Physics, University of Illinois, Chicago
[2] Department of Neurobiology, University of Chicago
[3] Argonne National Laboratory, Lemont, IL
[4] Department of Chemistry, University of Chicago
[5] James Franck Institute, University of Chicago
[6] Leiden Institute of Physics, Leiden University
[7] IBM T.J. Watson Research Center

corresponding authors: sbking@uchicago.edu, bobbykasthuri@uchicago.edu

1 Abstract

Detailing the physical basis of neural circuits with large-volume serial electron microscopy (EM), 'connectomics', has emerged as an invaluable tool in the neuroscience armamentarium. However, imaging synaptic resolution connectomes is currently limited to either transmission electron microscopy (TEM) or scanning electron microscopy (SEM). Here, we describe a third way, using photoemission electron microscopy (PEEM) which illuminates ultra-thin brain slices collected on solid substrates with UV light and images the photoelectron emission pattern with a wide-field electron microscope. PEEM works with existing sample preparations for EM and routinely provides sufficient resolution and contrast to reveal myelinated axons, somata, dendrites, and sub-cellular organelles. Under optimized conditions, PEEM provides synaptic resolution; and simulation and experiments show that PEEM can be transformatively fast, at Gigahertz pixel rates. We conclude that PEEM imaging leverages attractive aspects of SEM and TEM, namely reliable sample collection on robust substrates combined with fast wide-field imaging, and could enable faster data acquisition for next-generation connectomics.

2 Introduction

A confluence of advances in 3D EM imaging, sample preparation, and algorithms has enabled the exhaustive mapping of how neurons connect in large volumes of brain – connectomics. Connectomics has emerged as an invaluable tool in the neuroscience toolbox and connectomes of

cortex, retina, songbird HVC, zebrafish larva, and entire fly brains have helped discover principles of brain functions that could not have been revealed in any other way [1, 2, 3, 4, 5, 6, 7, 8]. These datasets are also inherently valuable as public repositories for future investigations by the broader neuroscience community [9, 10]. Thus, there is only increased demand for even larger 3D EM datasets. The next leap in connectomics will be reconstructing full neural circuits in mammalian brains. But to make that leap, large-volume connectomes need to be cheaper and faster. A 50-100 fold drop in the price of a 'connectomic voxel' could revolutionize connectomics, the way a 50-100 fold reduction in the cost of DNA sequencing [11] placed large-scale DNA analysis at the core of modern biology. However, all EM connectomic reconstructions use either transmission electron microscopy (TEM) or scanning electron microscopy (SEM) [12], which have limitations in the reliable automated serial pickup of ultrathin brain slices (UTBS), or in acquisition costs, respectively.

In this paper, we investigated whether photoemmission electron microscopy (PEEM) would be a third option. Photoemission electron microscopes are commercially available, are routinely used in chemistry and surface physics [13, 14, 15, 16, 17] and have been used since the 1970s for biological imaging [18, 19], and even to image neurons in culture [20]. PEEM uses wide-field UV illumination to emit photoelectrons from materials, often metals, and captures variations in the resulting electron emission pattern with standard electron optics [21] (**Figure 1**). Emitted electrons are accelerated (usually to 10 keV to 20 keV) and magnified onto an electron detector. Commercial PEEMs can have resolution capabilities of less than 15 nm, which is suitable for synaptic connectomics [1]. There are also PEEM detectors available that capture data at multi-GHz pixel rates, making a fast PEEM for connectomics plausible. Here, we report the first study of PEEM imaging of ultrathin brain slices prepared for standard electron microscopy.

3 Results

As PEEM is usually done on flat conductive substrates, we manually picked up 60 nm brain sections that had been prepared for EM-based connectomics [22] on a square-centimeter-sized piece of silicon with native oxide termination, coated with a 50 nm layer of gold and glow-discharged to increase hydrophilicity and adhesiveness of brain sections. We found that UTBS could be reliably imaged in a PEEM with a mercury arc lamp that emits most of its UV light at 254 nm [23]. We were able to identify biological features readily observed in standard connectomic datasets including cellular features (e.g., somata, blood vessels, dendrites, and myelinated axons) and sub-cellular features (e.g., mitochondria, endoplasmic reticulum, nuclear membrane, and nucleolus), see **Figure 2**. PEEM imaging is also relatively free of distortions – we tiled multiple overlapping PEEM fields of view (FOV) and collected and aligned small stacks of PEEM images of serial sections(**Figure 3**). In such stacks, we traced the processes of myelinated axons, dendrites, and glia, demonstrating that PEEM works in 3D and can be used to reconstruct projectomes [24]. Lastly, we acquired a 15 nm resolution PEEM image where synapses could be clearly identified with individual, putative $\sim$40 nm diameter, synaptic vesicles visible (**Figure 4**), meaning PEEMs can deliver sufficient resolution for full connectomic circuit reconstruction.

We next explored whether PEEM imaging could be fast, potentially at Gigahertz acquisition rates. For the results shown in this study, Hg arc lamps were used to illuminate the sample but the low photon flux necessitates long integration times, i.e., minutes, which is too slow to image large

volumes with PEEM. An obvious upgrade would be to illuminate instead with Ultraviolet-C lasers which produce a photon flux over 10,000 times higher than arc lamps. Thus, we investigated the compatibility of UTBS with laser-based illumination.

We first conservatively estimated that at most 3 million photons are needed to elicit an electron (see **Methods**). We then measured the emissivity ratio of lightly osmium-stained cytoplasm to more heavily osmium-stained structure like mitochondria in Figure 2 and found a ratio of 2.7 $\pm$ 0.2. A 0.5 W 244 nm laser produces a flux of 6.1×10^{-17} photons per second and using the Rose contrast criterion [25], we concluded that such a laser would provide enough signal to support connectomic resolution imaging at a pixel rate of over 2 GHz. Notably, such lasers are commercially available.

We next asked whether such illumination, a 0.5 W laser focused onto a field of view (FOV) tens of microns wide, would damage UTBS. We measured the absorption of UTBS for a range of wavelengths (see Methods). Interestingly, the absorption in epoxy has a local minimum at 251 nm, which we noted as a potential wavelength for future PEEM work (see Discussion). Using this absorption data, we simulated the heating of a 40 nm thick brain slice on a reflective silicon substrate with a 40 µm $\times$ 40 µm FOV by a 0.5 W laser and found that this would heat the epoxy by only 21.6 K (**Supplementary Table 1**). We experimentally confirmed (using a 266 nm Raman continuous-wave laser) that a slice of epoxy on silicon can withstand the equivalent photon flux (0.31 mW/µm^2) without epoxy burn-off. In anticipation of future development of more powerful UV-C lasers, we also simulated UTBS on more heat-conductive substrates,copper and diamond, and found that they would support 1.6 W and 3.9 W lasers respectively without going beyond the UTBS heating described above. This would allow PEEMs to image at 6.4 and 15.6 Gigahertz pixel rate, respectively. Lastly, we simulated space charging, i.e., whether electrons emitted at Gigahertz rates from 10s of microns FOVs would potentially interact with each other, repulsing each other and reducing the effective resolution of PEEM imaging, which has been cited as a potential limit of PEEM imaging speed [26, 27]. We found that PEEM imaging with a 0.5 W continuous-wave laser and a 40 µm $\times$ 40 µm FOV deflected no electrons more than 1 nm. At 15.6 GHz pixel rate, 0.2 % of the electron would deflect more than that (**Supplementary Figure 1**) which is still compatible with resolutions required for connectomes. We conclude that connectomic PEEM imaging of UTBS with a suitable laser would be well-resolved and fast.

4 Discussion

Here we describe the first successful imaging of UTBS using PEEM at synaptic resolution. Furthermore, we demonstrate the plausibility of using UV-C laser illumination of UTBS to significantly increase PEEM imaging rates, exceeding state-of-the-art SEM and TEM techniques used for connectomic imaging of brains. Below we discuss future directions on how to make large-volume connectomic PEEM imaging possible, with the acquisition of the data for a whole mouse brain within reach.

4.1 A PEEM mouse brain

An adult mouse brain, conservatively assumed to be 1 cm^3, imaged at 15 nm isotropic resolution, as demonstrated above, would result in 2.96×10^{17} voxels. A single PEEM using CW UV laser

illumination, imaging non-stop at 2 Gigahertz pixel rate, would take approximately five years to finish that acquisition. UTBS can be easily distributed across multiple PEEMs, decreasing the time to map a mouse brain proportionately to the number of PEEMs used. A machine with a pixel throughput of 2 GHz is likely feasible given the analyses above and would be faster than current approaches using TEMs or SEMs with a potentially significant reduction in price.

A PEEM connectome of a mouse brain will require automating both the collection and imaging of 1000s of UTBS. Since PEEM has similar requirements to SEM imaging, i.e., section flatness, conductive substrates, and maximizing UTBS density, we argue existing state-of-the-art approaches for automated collection of serial UTBS on conductive substrates, such as automated collection on tape (ATUM) [28] and collection on silicon, MagC [29] could be used to scale the number of samples for PEEM.

We end with noting that illuminating UTBS with photons instead of electrons opens up the space of sample preparation for PEEM imaging. It is plausible that different sample preparations may be even more suitable for PEEM and that combinations of existing EM stains or entirely new stains could increase contrast. Also, for each contrast agent candidate, higher throughput could be achieved by identifying the optimal excitation wavelength. Lastly, PEEM is thought of as a surface imaging technique, sampling only the top few nanometers [30]. This makes it an interesting match for Gas Cluster Ion Milling [31]. Stain, laser wavelength, and milling thickness are to be matched to extract the maximum amount of information from the sample in minimum time. In summary, further exploration of PEEM as a connectomic technique can only increase its capability and open new pathways for providing large-volume circuit mapping.

5 Methods

5.1 Sample Preparation

Mouse brain sections were prepared for PEEM imaging following the same protocol used for standard SEM preparation using multiple rounds of osmium tetroxide staining [22]. In brief, the mouse was perfused transcardially to preserve the ultrastructure. The mouse brain was surgically removed and fixed, and a vibratome-sectioned brain slice (200 µm to 300 µm) was stained with successive rounds of osmium tetroxide, potassium ferrocyanide, uranyl acetate, and lead nitrate, before ethanol dehydration and embedding with EPON resin. Resin-encapsulated brain was then sliced using an ultramicrotome to 40-80 nm-thick UTBS, which were picked up on a Si substrate with native oxide coated with 50 nm of polycrystalline gold and glow-discharged.

5.2 Photoemission electron microscopy

The UTBS on the substrate is illuminated using a broadband Hg arc lamp with a short-pass filter allowing photons with energies greater than 4.43 eV (280 nm) to focus on the sample, shown schematically in Figure 1. The resulting photoelectrons are imaged with a photoemission electron microscope manufactured by Focus GmbH (Figure 2) and SPECS GmbH (Figure 3 and 4, aberration-corrected microscope). The typical exposure time for one image is hundreds of seconds. High-resolution images are obtained by integrating the same region of interest (ROI) to improve signal-to-noise. To estimate how many photons would be required to elicit an electron,

we used a pulsed laser with a wavelength of 244 nm and known flux, and acquired a PEEM image of a 60 nm brain slice deposited on gold. We estimated the amount of electrons collected by measuring the SNR ratio and calculating from that shot noise measurement back to the number of electrons collected.

5.3 Image processing

2D image montaging was performed in FIJI (ImageJ) using the Grid/Collection stitching plugin. PEEM image stacks were 3D-aligned using AlignTK (https://mmbios.pitt.edu/aligntk-home). To achieve the necessary contrast of UTBS in PEEM, multiple images of the same ROI were captured which introduced drift to the set of images, presumably from instabilities in the stage. Therefore, two people (G.W. and K.M.B.) independently visually inspected the series of images to estimate the pixel drift which was corrected by shifting the images by the estimated pixel drift. Lastly, a maximum intensity projection was generated from the drift-corrected series to produce the final PEEM images.

5.3.1 Manual annotations and resolution measurement

Manual 3D annotation was done using VAST [32]. To measure the resolution of images such as the one shown in Figure 4, 10 membrane-cytoplasm transitions of drift-corrected images were inspected and the distance between the 16 % and 84 % intensity levels determined. Of these measurements, the 25th percentile was reported.

5.4 Space charging simulations

Electrons were simulated to be emitted from a 40 µm $\times$ 40 µm substrate with a spatial distribution according to an existing low-noise EM image (10 nm pixel size) from a UTBS of neuropil. They were given an isotropic energy distribution with a standard deviation of 2 eV. After emission, the electrons were subjected to a homogeneous electric field of 15 kV/mm. In each 10 fs time step of the simulation, the Coulomb interaction of each pair of in-flight electrons was calculated and applied to the electrons. Once an electron had a distance greater 1 mm from the sample, it was removed from the simulation. This process was repeated until 5000 electrons had been removed that were not affected by simulation ramp-up effects. Then, using their final position and angle, for each electron it was determined which position the electron optic would reconstruct the electron to have come from and this was compared to the actual origin. Throughput was calculated using the Rose contrast criterion [25].

6 Acknowledgments

We thank Vitali Prakapenka and Stella Chariton for help with the laser experiments. We thank Peter Littlewood, Winfried Denk, Rolf Koenenkamp, S. Murray Sherman, John Maunsell and Mark Schnitzer for helpful discussions and/or comments on the manuscript. We thank Janek Rieger, Jerzy Sadowski, Oliver Schaff, Chris Nicholson, Lisa van Leeuwen, Marcel Hesselberth, Helder Marchetto, and Pupa Gilbert for supporting this project. This work was partially supported

by the University of Chicago Materials Research Science and Engineering Center, which is funded by the National Science Foundation under award number DMR-2011854 and DMR-1420709. This work made use of the shared facilities at the University of Chicago Materials Research Science and Engineering Center, supported by National Science Foundation under award number DMR-2011854. R.L. acknowledges support from a MRSEC-funded graduate research fellowship (DMR-1420709). S.B.K. acknowledges start-up funding support from the University of Chicago and the Neubauer Family Assistant Professors Program. L.L. acknowledges support from the University of Chicago Neuroscience Early Stage Scientist Training Program 1R25NS117360. Part of this project has received funding from the European Union's Horizon 2020 research and innovation program under grant agreement No 101017902.

7 Data availability

Raw data and code will be made available on Zenodo and GitHub upon publication.

References

[1] K. L. Briggman, M. Helmstaedter, and W. Denk. "Wiring specificity in the direction-selectivity circuit of the retina". In: *Nature* 471.7337 (Mar. 2011), pp. 183–188. ISSN: 1476-4687. DOI: 10.1038/nature09818.

[2] J. R. Anderson et al. "Exploring the retinal connectome". In: *Molecular Vision* 17 (Feb. 2011), pp. 355–379. ISSN: 1090-0535.

[3] D. D. Bock et al. "Network anatomy and in vivo physiology of visual cortical neurons". In: *Nature* 471.7337 (Mar. 2011), pp. 177–182. ISSN: 1476-4687. DOI: 10.1038/nature09802.

[4] N. Kasthuri et al. "Saturated Reconstruction of a Volume of Neocortex". In: *Cell* 162.3 (July 2015), pp. 648–661. ISSN: 1097-4172. DOI: 10.1016/j.cell.2015.06.054.

[5] J. Kornfeld et al. "EM connectomics reveals axonal target variation in a sequence-generating network". In: *eLife* 6 (Mar. 2017), e24364. ISSN: 2050-084X. DOI: 10.7554/eLife.24364.

[6] F. Svara et al. "Automated synapse-level reconstruction of neural circuits in the larval zebrafish brain". In: *Nature Methods* 19.11 (Nov. 2022), pp. 1357–1366. ISSN: 1548-7105. DOI: 10.1038/s41592-022-01621-0.

[7] M. Winding et al. "The connectome of an insect brain". In: *Science* 379.6636 (Mar. 2023), eadd9330. DOI: 10.1126/science.add9330.

[8] S.-y. Takemura et al. *A Connectome of the Male Drosophila Ventral Nerve Cord*. June 2023. DOI: 10.1101/2023.06.05.543757.

[9] S. Dorkenwald et al. "FlyWire: online community for whole-brain connectomics". In: *Nature Methods* 19.1 (Jan. 2022), pp. 119–128. ISSN: 1548-7105. DOI: 10.1038/s41592-021-01330-0.

[10] R. Hider et al. "The Brain Observatory Storage Service and Database (BossDB): A Cloud-Native Approach for Petascale Neuroscience Discovery". In: *Frontiers in Neuroinformatics* 16 (2022). ISSN: 1662-5196.

[11] A. v. Bubnoff. "Next-Generation Sequencing: The Race Is On". In: *Cell* 132.5 (Mar. 2008), pp. 721–723. ISSN: 0092-8674, 1097-4172. DOI: 10.1016/j.cell.2008.02.028.

[12] L. M. Collinson et al. "Volume EM: a quiet revolution takes shape". In: *Nature Methods* 20.6 (June 2023), pp. 777–782. ISSN: 1548-7105. DOI: 10.1038/s41592-023-01861-8.

[13] P. P. Joshi et al. "Nanoimaging of the Edge-Dependent Optical Polarization Anisotropy of Black Phosphorus". In: *Nano Letters* 22.8 (Apr. 2022), pp. 3180–3186. ISSN: 1530-6984. DOI: 10.1021/acs.nanolett.1c03849.

[14] Y. Dai et al. "Plasmonic topological quasiparticle on the nanometre and femtosecond scales". In: *Nature* 588.7839 (Dec. 2020), pp. 616–619. ISSN: 1476-4687. DOI: 10.1038/s41586-020-3030-1.

[15] G. Spektor et al. "Revealing the subfemtosecond dynamics of orbital angular momentum in nanoplasmonic vortices". In: *Science* 355.6330 (Mar. 2017), pp. 1187–1191. DOI: 10.1126/science.aaj1699.

[16] R. M. Tromp et al. "A new aberration-corrected, energy-filtered LEEM/PEEM instrument. I. Principles and design". In: *Ultramicroscopy* 110.7 (June 2010), pp. 852–861. ISSN: 0304-3991. DOI: 10.1016/j.ultramic.2010.03.005.

[17] T. Schmidt et al. "Double aberration correction in a low-energy electron microscope". In: *Ultramicroscopy* 110.11 (Oct. 2010), pp. 1358–1361. ISSN: 0304-3991. DOI: 10.1016/j.ultramic.2010.07.007.

[18] E. Bauer. "A brief history of PEEM". In: *Journal of Electron Spectroscopy and Related Phenomena*. Photoelectron microscopy, Time resolved pump-probe PES 185.10 (Oct. 2012), pp. 314–322. ISSN: 0368-2048. DOI: 10.1016/j.elspec.2012.08.001.

[19] R. Könenkamp et al. "5.4nm spatial resolution in biological photoemission electron microscopy". In: *Ultramicroscopy* 110.7 (June 2010), pp. 899–902. ISSN: 0304-3991. DOI: 10.1016/j.ultramic.2010.04.005.

[20] G. d. Stasio et al. "High-Resolution Photoelectron Microimaging of Neuron Networks". In: *Europhysics Letters* 16.4 (Sept. 1991), p. 411. ISSN: 0295-5075. DOI: 10.1209/0295-5075/16/4/016.

[21] G. F. Rempfer, W. P. Skoczylas, and O. Hayes Griffith. "Design and performance of a high-resolution photoelectron microscope". In: *Ultramicroscopy* 36.1 (May 1991), pp. 196–221. ISSN: 0304-3991. DOI: 10.1016/0304-3991(91)90151-U.

[22] Y. Hua, P. Laserstein, and M. Helmstaedter. "Large-volume en-bloc staining for electron microscopy-based connectomics". In: *Nature Communications* 6.1 (Aug. 2015), p. 7923. ISSN: 2041-1723. DOI: 10.1038/ncomms8923.

[23] C. J. Sansonetti, M. L. Salit, and J. Reader. "Wavelengths of spectral lines in mercury pencil lamps". In: *Applied Optics* 35.1 (Jan. 1996), pp. 74–77. ISSN: 2155-3165. DOI: 10.1364/AO.35.000074.

[24] N. Kasthuri and J. W. Lichtman. "The rise of the 'projectome'". In: *Nature Methods* 4.4 (Apr. 2007), pp. 307–308. ISSN: 1548-7105. DOI: 10.1038/nmeth0407-307.

[25] A. Rose. *Vision: Human and Electronic*. Springer US, 1974. ISBN: 978-0-306-30732-4.

[26] A. Locatelli et al. "Image blur and energy broadening effects in XPEEM". In: *Ultramicroscopy* 111.8 (July 2011), pp. 1447–1454. ISSN: 0304-3991. DOI: 10.1016/j.ultramic.2010.12.020.

[27] D. Wilson et al. "On space charge effects in laboratory-based photoemission electron microscopy using compact gas discharge extreme ultraviolet sources". In: *New Journal of Physics* 22.10 (Oct. 2020), p. 103019. ISSN: 1367-2630. DOI: 10.1088/1367-2630/abbc29.

[28] V. Baena et al. "Serial-section electron microscopy using automated tape-collecting ultramicrotome (ATUM)". In: *Methods in Cell Biology* 152 (2019), pp. 41–67. ISSN: 0091-679X. DOI: 10.1016/bs.mcb.2019.04.004.

[29] T. Templier. "MagC, magnetic collection of ultrathin sections for volumetric correlative light and electron microscopy". In: *eLife* 8 (July 2019), e45696. ISSN: 2050-084X. DOI: 10.7554/eLife.45696.

[30] W. A. Houle et al. "Depth of information in photoelectron microscopy". In: *Ultramicroscopy* 7.4 (Jan. 1982), pp. 371–380. ISSN: 0304-3991. DOI: 10.1016/0304-3991(82)90261-3.

[31] K. J. Hayworth et al. "Gas cluster ion beam SEM for imaging of large tissue samples with 10 nm isotropic resolution". In: *Nature Methods* 17.1 (Jan. 2020), pp. 68–71. ISSN: 1548-7105. DOI: 10.1038/s41592-019-0641-2.

[32] D. R. Berger, H. S. Seung, and J. W. Lichtman. "VAST (Volume Annotation and Segmentation Tool): Efficient Manual and Semi-Automatic Labeling of Large 3D Image Stacks". In: *Frontiers in Neural Circuits* 12 (2018). ISSN: 1662-5110.

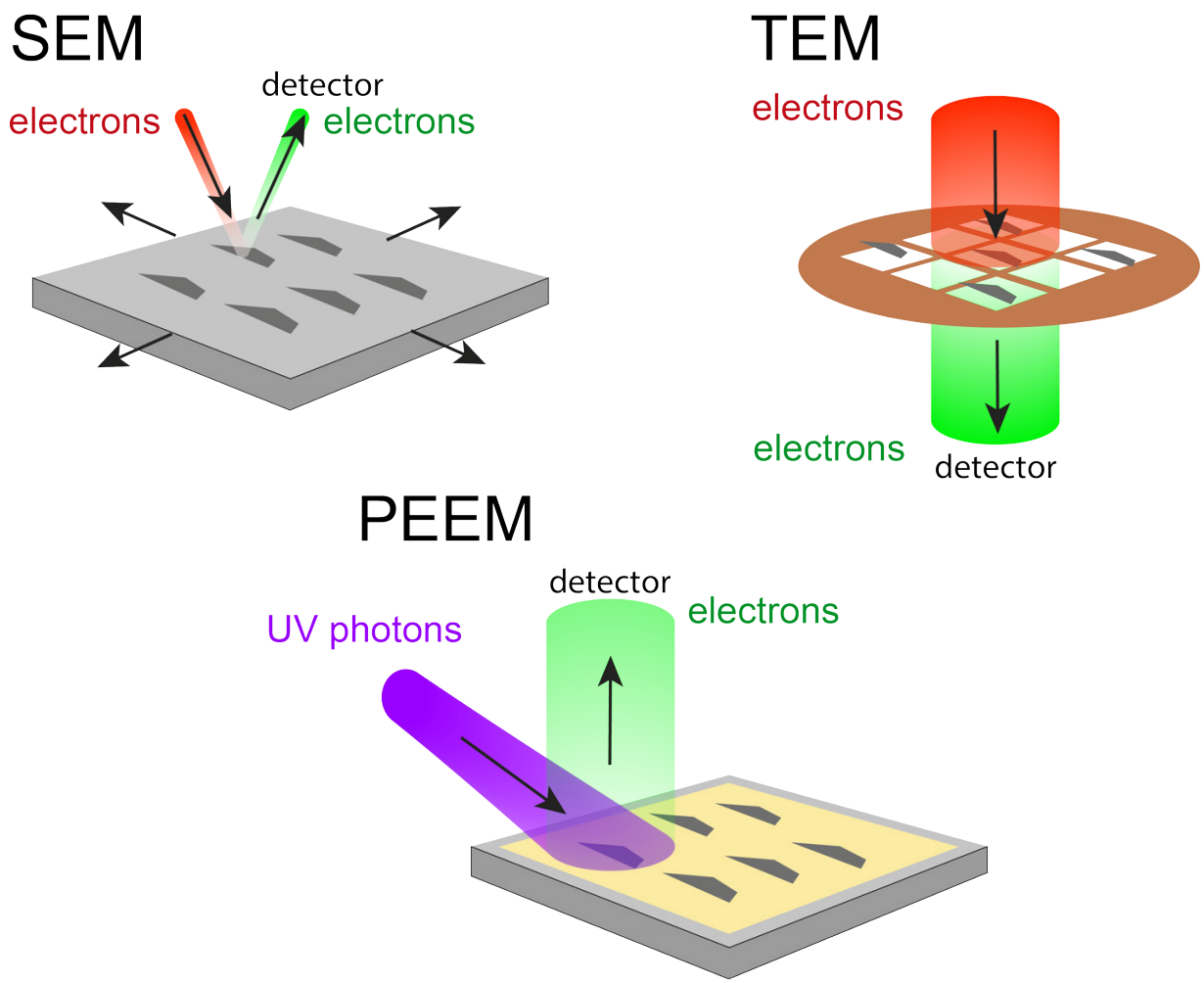

Figure 1: Photoemission electron microscopy (PEEM) combines the advantages of SEM and TEM for high-throughput volume electron microscopy (vEM). SEM allows for more reliable section collection on solid substrates, but is slower due to the inherently sequential nature of scanning microscopy. TEM is wide-field imaging and fast but samples are collected onto grids with thin fragile substrates, increasing the complexity of collecting thousands of UTBS. PEEM combines the best of both, imaging samples on solid substrates with wide-field imaging technique, and thus has the potential to supersede these techniques and enable the next generation of large-volume connectomes.

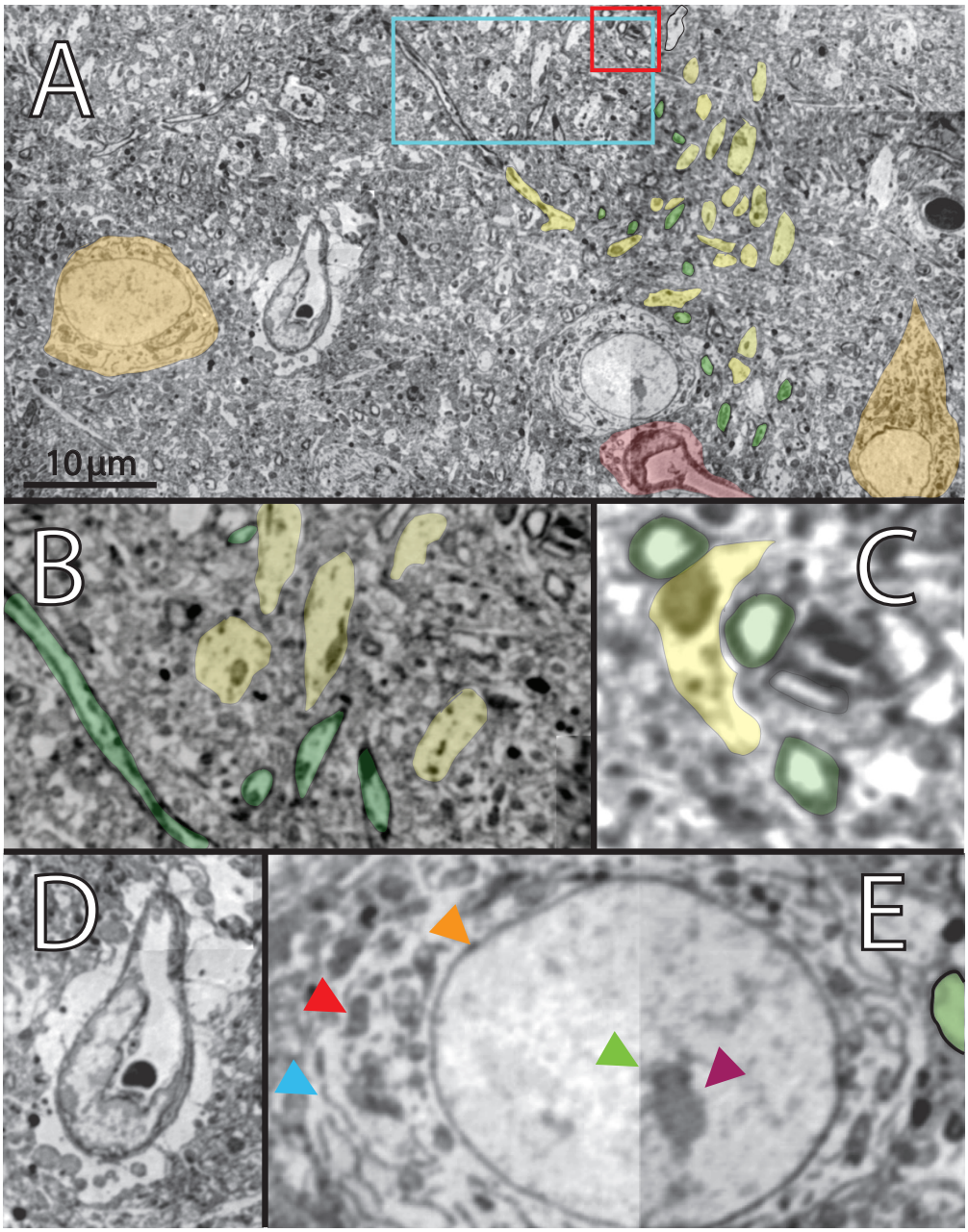

Figure 2: PEEM reveals cellular and subcellular features similar to standard EM data. A) a 60 nm UTBS was imaged over 9 overlapping fields of view (FOV) spanning 72 µm × 37 µm and algorithmically stitched together. PEEM images clearly show different neurobiological features commonly found in EM datasets including somata (orange), blood vessels (red), dendrites (yellow), and individual myelinated axons (green). **B)** Zoom in from A (light blue box) showing close-up of individual dendrites (yellow) and myelinated axons (green). **C)** Zoom in from B (red box) showing further detail of individual dendrites (yellow) and myelinated axons (green). **D)** Representative example of a blood vessel with the processes of an astrocyte making a putative neurovascular unit. **E)** Representative example of a neuronal soma with clearly visible mitochondria (red arrowhead), endoplasmic reticulum (light blue arrowhead), nucleolus (purple arrowhead), and nuclear membrane (orange arrowhead). Green arrowhead shows stitch line between two FOVs.

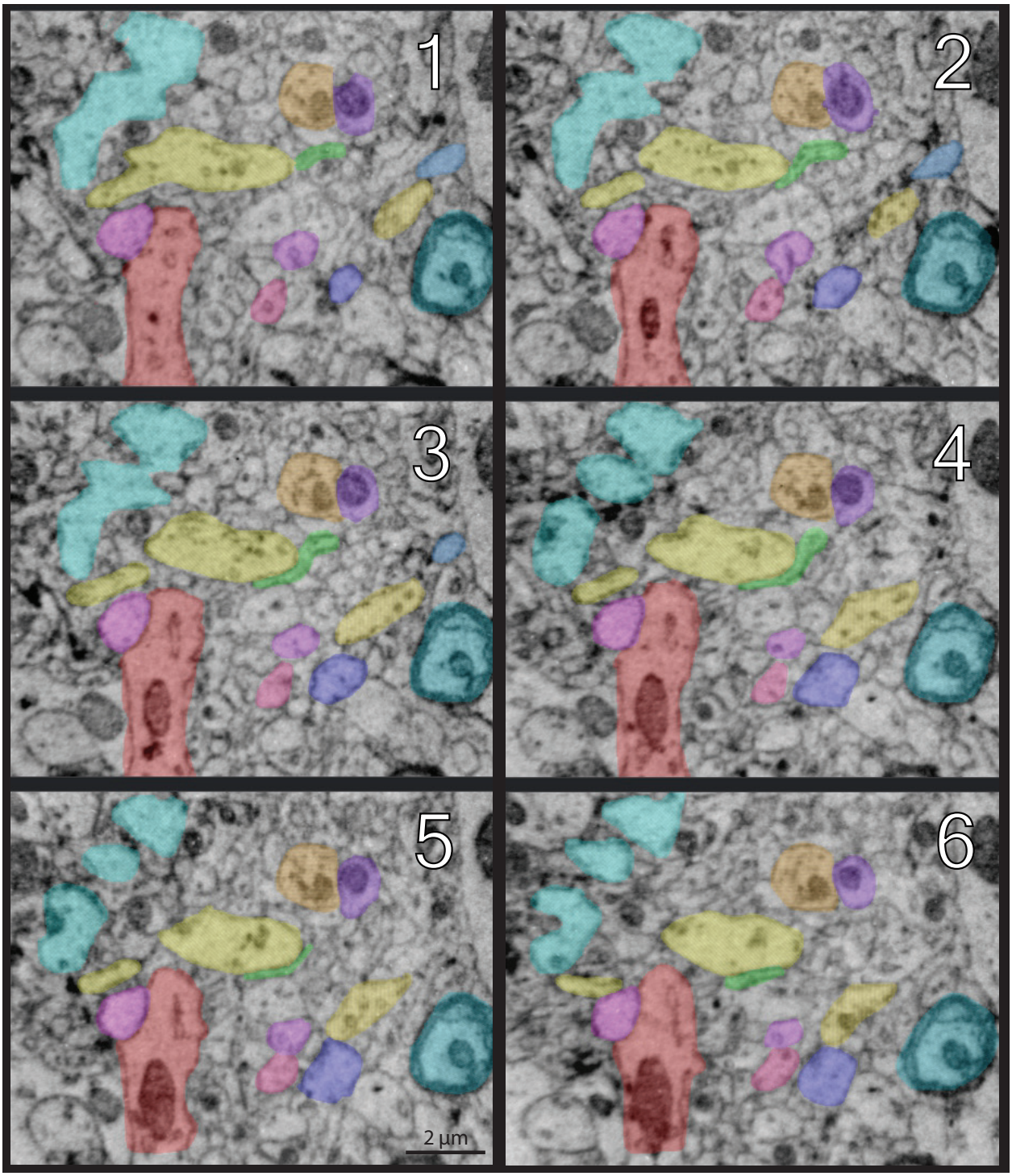

Figure 3: Tracing neurites in a serial stack of UTBS imaged with PEEM. Shown are images of a serial stack of UTBS, 40 nm thick, imaged with medium-resolution PEEM. The stack was aligned using AlignTK. Multiple neurological features can be manually traced through the stack including dendrites of varying size, myelinated axons, and glia across 6 sections.

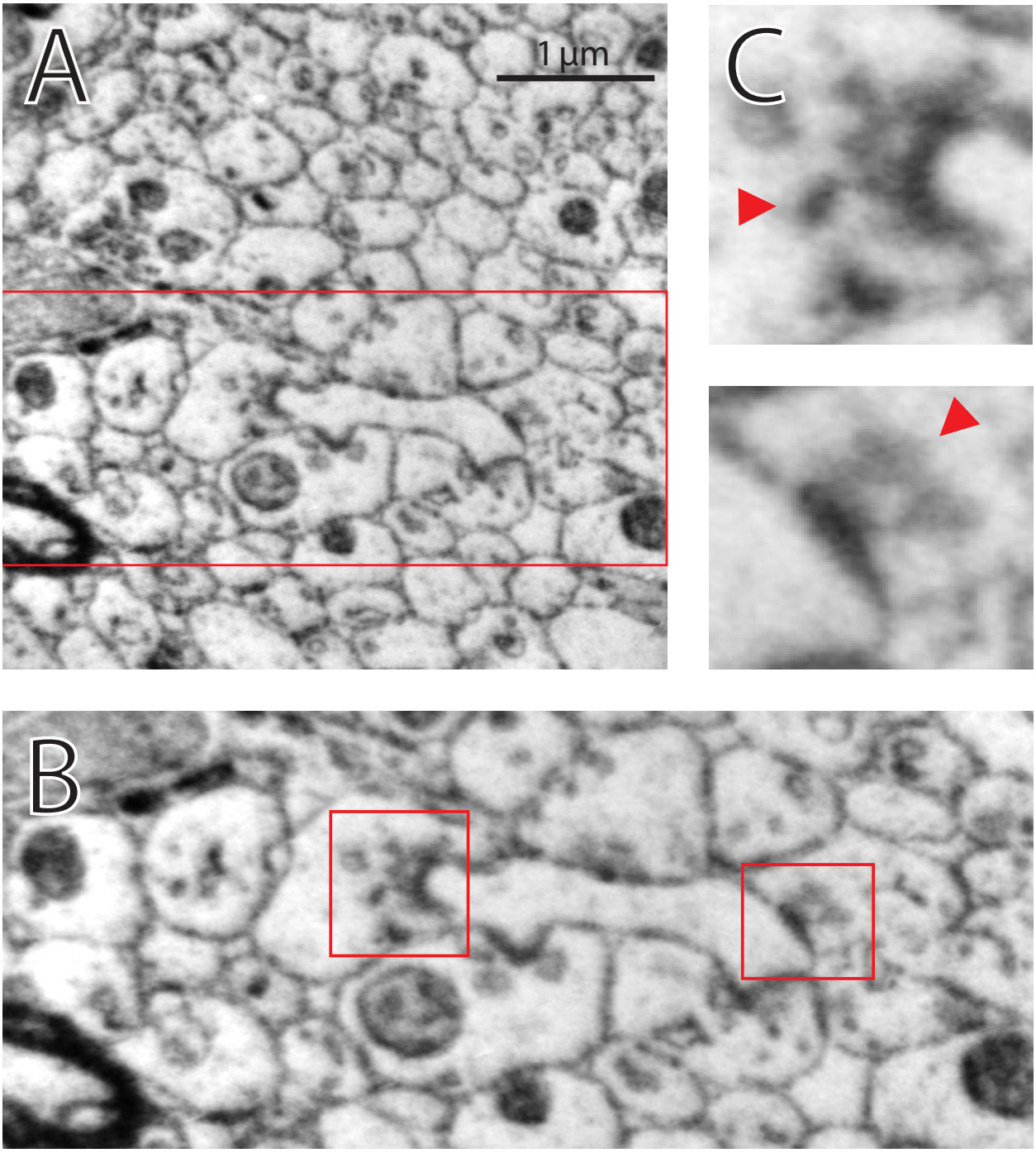

Figure 4: PEEM can achieve synaptic resolution. A) PEEM image of a UTBS at 15 nm resolution. B) Zoom in from A (red rectangle) showing multiple synapses (red squares) as evidenced by the presence of a post-synaptic densities (PSD) and pre-synaptic vesicle clouds. C) Zoom in from B (red squares) of two synapses with individual pre-synaptic vesicles visible (red arrowheads).